Coupling of disulfide bond and distal histidine dissociation in human ferrous cytoglobin regulates ligand binding

Penny Beckerson, Brandon J. Reeder* and Michael T. Wilson
School of Biological Sciences, University of Essex, Wivenhoe Park, Colchester, Essex, CO4 3SQ,

*Corresponding author email: reedb@essex.ac.uk

Short title: Disulfide bond in ferrous cytoglobin

ABSTRACT: Earlier kinetics studies on cytoglobin did not assign functional properties to specific structural forms. Using defined monomeric and dimeric forms and cysteine mutants we show that an intramolecular disulfide bond (C38-C83) alters the dissociation rate constant of the intrinsic histidine (H81) (~1000 fold), thus controlling binding of extrinsic ligands. Through time-resolved spectra we have unequivocally assigned CO binding to hexa- and penta-coordinate forms and have made direct measurement of histidine rebinding following photolysis. We present a model that describes how the cysteine redox state of the monomer controls histidine dissociation rate constants and hence extrinsic ligand binding.

Keywords: Cytoglobin; carbon monoxide; flash photolysis; ferrous; biphasic; distal histidine; monomer; dimer; disulfide; cysteine

Abbreviations: Cygb, cytoglobin; $monomer_{S\text{-}S}$, cytoglobin monomer with intramolecular disulfide bond; $monomer_{S\text{-}H}$, cytoglobin monomer with sulfhydryl groups; $dimer_{S\text{-}S}$, cytoglobin dimer with intermolecular disulfide bond.

Highlights

- An intramolecular disulfide bond in monomeric cytoglobin modulates CO binding.
- Histidine on and off rates for the different forms of cytoglobin were determined.
- We identify two forms of the hexacoordinate monomeric protein.
- A model is presented describing CO binding to the different forms of cytoglobin.

Introduction

Cytoglobin (Cygb) is a relatively new member of the vertebrate hemoglobin superfamily[1,2] and displays hexacoordination (His-Fe-His) similar to neuroglobin [3-6]. Binding of exogenous ligands is therefore competitive with the endogenous histidine, giving multiphasic binding kinetics following flash photolysis; behavior that has been reported in other hexacoordinate globins such as rice non-symbiotic hemoglobin [7,8].

Previously Cygb has been shown to be an intermolecular disulfide linked homo-dimer, however recent studies have identified a monomeric form and also the presence of an internal disulfide bond [9,10]. The presence of this bond (C38-C83) has been shown to affect ligand binding kinetics and affinities [10] and other characteristics including the ability to interact with lipids in the ferric form [11]. In our previous stopped-flow studies we proposed that the formation of an intramolecular disulfide bond leads to movement of helices B and E, which results in a change in the distal histidine dissociation rate constant. Lechauve *et al.* (2010) have previously investigated the functional properties of Cygb and have related ligand recombination rates, following flash photolysis, to conformations of the protein that depend on the absence or presence of disulfide bonds. They also conclude that the histidine dissociation rate constant is decreased in the presence of dithiothreitol, which disrupts disulfide bonds.

In this study we extend our previous work and that of Lechauve *et al.* (2010) by undertaking further laser photolysis experiments. The use of defined monomeric and dimeric forms and mutation of specific cysteine residues (C38) has demonstrated that the intramolecular disulfide bond between C38 and C83 controls the dissociation rate constant of the intrinsic histidine (H81) from the central iron. Through this mechanism control of binding extrinsic ligands such as CO is exerted. Our conclusions are in overall qualitative agreement with Lechauve *et al.* (2010) but we report some important quantitative differences in the values for CO binding rate constants and histidine binding and dissociation rate constants. Through time-resolved spectra we have assigned unequivocally CO binding to hexa- and penta-coordinate forms and have made direct measurement of histidine rebinding following photolysis. We present a model that summarizes our conclusions and those of earlier work, which incorporates changes in ligand affinities, ligand binding rate constants and distal histidine association and dissociation rate constants controlled by the cysteine residue redox state in the monomeric form [9,10,12].

Materials and methods

Cytoglobin engineering, expression and purification

Human cytoglobin was expressed and purified as previously described [11,13]. The monomeric fraction with an internal disulfide bond ($monomer_{S\text{-}S}$), dimeric fraction with intermolecular disulfide ($dimer_{S\text{-}S}$) and polymeric fraction were separated using G-75 Superdex column (600 mm x 16 mm, GE Healthcare) equilibrated with 0.1 M sodium phosphate buffer (pH 7.4) with an AKTA purification system. Fractions were collected corresponding to the absorbance peaks at 280 nm. The mutated C38R Cygb was prepared as previously described with the monomeric fractions used and is subsequently referred to as $monomer_{S\text{-}H}$ [11]. Monomeric distal histidine mutant of Cygb (H81Y), which showed penta-coordination of the heme iron, was generated by site directed mutagenesis and expressed and purified using the same protocol as the WT.

Preparation of the ferrous protein

It has been previously shown that the disulfide bond in Cygb is reduced by sodium dithionite with a half time of ~2000 s [11]. Therefore samples of ferrous Cygb, prepared by addition of a slight excess of dithionite to degassed protein solution, were used within approximately 5 minutes. Our previous studies have shown that there is negligible change in CO binding kinetics as a result of disulfide bond reduction over this time period [11].

Carbon monoxide titrations

A solution of CO was prepared by the equilibration of 0.1 M sodium phosphate buffer (pH 7.4) with 1 atmosphere of CO at 20 °C to give a solution of ~ 1 mM CO. The precise concentration of CO was calculated by a titration against ferrous myoglobin, which binds at a 1:1 stoichiometry. A sealed quartz cuvette with no headspace was filled with degassed 0.1 M sodium phosphate buffer (pH 7.4). Ferrous Cygb $monomer_{S\text{-}S}$, $monomer_{S\text{-}H}$ and $dimer_{S\text{-}S}$ were diluted to a concentration of 5 µM and titrated with the CO solution using a micrometer screw-gage AGLA syringe with 5 µL addition giving ~ 0.5 µM CO additions. Upon each addition changes in absorbance between 350-600 nm were recorded. Data was fitted, using Graphpad 6.0, to equation 1 below as previously reported [13], where $[P_T]$ is the total protein concentration, [S] is the total ligand concentration (CO) and K is the dissociation constant.

$$Y = \frac{([P_T] + [S] + K) - \sqrt{([P_T] + [S] + K)^2 - 4([P_T][S])}}{2[P_T]}$$

Equation 1

Carbon monoxide flash photolysis

An Applied Photophysics LKS80 laser flash photolysis spectrometer equipped with a monochrometer and photomultiplier was used to measure changes in absorbance following laser dissociation of CO from ferrous $monomer_{S\text{-}S}$, $monomer_{S\text{-}H}$ and $dimer_{S\text{-}S}$ Cygb (5 µM) in the presence of known concentrations of CO (0-500 µM). Averages of 6 flashes were recorded and observed rate constants calculated by using the ProKinetist software.

Difference spectra for each phase were calculated using changes in amplitudes at multiple wavelengths.

Results

Carbon monoxide titrations of ferrous monomer$_{S\text{-}S}$, dimer$_{S\text{-}S}$ and monomer$_{S\text{-}H}$ cytoglobin

Addition of saturating concentrations of CO to the 3 forms of ferro-Cygb (monomer$_{S\text{-}S}$, monomer$_{S\text{-}H}$ or dimer$_{S\text{-}S}$) led to the formation of a carbon monoxide complex, the spectral properties of which were independent of the Cygb form, i.e. Soret band at 423 nm, α and β peaks at 570 and 542 nm respectively, consistent with earlier observation [6,11] (Figure 1 inset). Figure 1 shows the results of CO titrations of each form in which small aliquots of a solution of CO were added to the ferrous protein. It is apparent from fitting these data (Equation 1) that the stoichiometry of binding is 1:1 (protein:CO) for each form. The affinities of the monomer$_{S\text{-}S}$ and monomer$_{S\text{-}H}$ are high ($K_D < 10^{-7}$ M) and could not be accurately determined from this method. The affinity of the dimer$_{S\text{-}S}$ is, however, significantly lower and we estimate from the fit a K_D of $3.3 \pm 0.9 \times 10^{-7}$ M. These results are consistent with those reported by Tsujino et al (2014).

Recombination of CO with ferrous monomer$_{S\text{-}S}$, dimer$_{S\text{-}S}$ and monomer$_{S\text{-}H}$ cytoglobin following laser photolysis

Previously reported stopped-flow studies investigating CO binding showed time courses for CO combination to monomer$_{S\text{-}S}$, dimer$_{S\text{-}S}$ and monomer$_{S\text{-}H}$ that were monophasic [11]. In contrast, following flash photolysis the time courses for CO recombination were biphasic (Figure 2). The two phases of the monomer$_{S\text{-}S}$ CO recombination exhibited different associated spectral changes. These are shown in Figure 2B and the optical changes of the fast phase are consistent with the binding of CO to the pentacoordinate form of the protein generated by the photolysis of the CO bond. The optical changes of the slower phase represent CO binding to the hexacoordinate form (His-Fe-His). This behavior is reminiscent of that displayed by hexacoordinate hemoglobins and is represented in Scheme 1 [8,14]. In this scheme the initial CO-complex (Scheme 1 - i) is photolysed to give the pentacoordinate species (ii). This penta-coordinate species may recombine in a second order process to form the initial CO-complex (i - k_{CO}). Alternatively the intrinsic distal histidine ligand binds to form a hexacoordinate species (iii), which subsequently is pulled through the equilibria back to the CO-complex (i – k_{slow}). This constitutes the slow phase as indicated by the spectral changes seen in Figure 2B. Consistent with this model, the fast phase displays a linear dependence on CO concentration and the relative amplitudes of the two processes are CO concentration dependent, reflecting the competition between the second order process of CO binding to the pentacoordinate species (k_{CO}) and the first order process (k_H) of histidine binding. Thus,

on increasing CO concentration the amplitude of the fast phase increases while that of the slow phase decreases (Figure 3). Interestingly, the rate constant of the slower phase also displays a (closely linear) CO concentration dependence (Figure 3) consistent with rapid equilibrium between the species ii and iii. The slope of the linear dependence on CO concentration in this case yields an apparent second order rate constant (k_{slow}), where (k_{slow})= k_{CO} (k_{-H}/k_H). Noteworthy, CO binding to the hexacoordinate form generated following laser flash photolysis is very much faster than CO binding to the hexacoordinate form followed by stopped-flow spectroscopy [11]. This type of behavior has been previously reported [9] and may be rationalized by presuming that the hexacoordinate form (iii) relaxes to a more stable hexacoordinate form (iv). This species (iv) is the starting point for stopped-flow experiments but is not populated to any significant degree in the photolysis experiments because species iii is rapidly removed and converted to the CO-complex (i).

Similar experiments undertaken using either the $dimer_{S\text{-}S}$ or $monomer_{S\text{-}H}$ yielded broadly similar results and are consistent with Scheme 1. Two phases of CO recombination were observed following photolysis, both displaying a CO concentration dependence (see figure 3). The rates however, were significantly lower than seen with the $monomer_{S\text{-}S}$ and are summarized in Table 1. However, within the errors of the data the CO dependency, although adequately fitted to a straight line, is also consistent with a hyperbolic dependence approaching a rate limit of ~0.5 s^{-1} for the dimer. One notable departure from this pattern was that at very low CO concentration (32 µM) histidine combination with the ferrous heme (k_H) significantly out-competed the CO binding to the pentacoordinate heme (k_{CO}). Under these circumstances the faster process now could be assigned, from the time-resolved difference spectra, to histidine binding to the iron (Figure 2D). The slower process, as with the $monomer_{S\text{-}S}$, is the recombination of CO to the hexacoordinate species (iii).

Discussion

Our results are in broad agreement with earlier work [9,12,15]. However, the use of defined forms of the protein, namely $monomer_{S\text{-}S}$, $dimer_{S\text{-}S}$ and $monomer_{S\text{-}H}$, has enabled us to describe more fully the mechanism through which ligand binding is regulated by the redox state of the cysteines in the protein. This mechanism is given in Scheme 1 and will form the basis of the following discussion. This model is a simplification and one might conceive that there are further mechanistic aspects that may be incorporated. However it is unlikely that further complication of the model will change our basic conclusion that the histidine dissociation rate constant is modulated by the absence or presence of the intramolecular disulfide bond in the monomeric species.

The amplitude of the fast phase of CO recombination is CO concentration dependent and this dependency follows a standard hyperbola function as shown in Figure 3B. The data were fitted to the following equation:

$$Y = \frac{[CO]}{K + [CO]} \text{(Equation 2)}$$

where Y is the fraction of the total amplitude of the processes following photolysis that occurs in the fast phase and K the phenomenological parameter denoting the [CO] at which half the total amplitude occurs in the fast phase. It is apparent that the maximum amplitude of the fast phase is different for the forms of Cygb used. This is most easily explained in terms of a larger fraction of geminate recombination occurring in the dimeric form, (and to a lesser extent monomer$_{S\text{-}H}$) suggesting that in this species CO egress is partially occluded. The hyperbolic amplitude dependence of the fast phase on CO concentration is to be expected, where this arises from the competition between a first order process (histidine recombination to the iron) and a second order process (CO recombination). If we neglect back reactions, an assumption that is reasonable given the affinity of CO for ferrous iron and the fact that the protein is hexacoordinate at equilibrium, then we may also express the fraction of the amplitude occurring in the fast phase (Y) as:

$$Y = \frac{k_{CO}[CO]}{(k_H + k_{CO}[CO])} \text{ (Equation 3)}$$

Combining equations 2 and 3 leads to a simple result, namely:

$$k_H = k_{CO}K \text{ (Equation 4)}$$

As we have values of k_{CO} and K from the fits to the data in Figures 3 we may calculate k_H for each protein species. The results from these calculations are given in Table 2. Furthermore, if we conclude from the linear dependency of the slow phase of CO recombination (see above) that, to a first approximation, $k_{slow} = k_{CO}\, K_H$ (where $K_H = k_H/k_{-H}$), then we may also calculate k_{-H}. These values are also provided in Table 2. The k_{-H} values calculated on this basis must be considered as lower estimates as the linearity of the dependency is not assured. This would lead our calculations (Table 2) to yield values of k_{-H} which are lower than those suggested from inspection of Figure 3C. For the dimer it is unlikely that the values in table 2 are different by more than a factor of 2 or 3. For the monomer$_{S\text{-}S}$ it would

appear that any plateau in the dependency must be above 500 s^{-1} rather than the 110 s^{-1} given in Table 2. These discrepancies arise from the limited CO concentration range available to us (0-500 µM) making it difficult to determine any limiting rate. Also the simplifying assumption that some back reactions may be considered to be negligible may be in error. In any case although he estimated values in Table 2 may be low the overall conclusions remain unchanged. The calculated value for k_H for the dimer and monomer$_{S-H}$ find support from the laser photolysis data conducted at very low CO concentrations where we observed directly recombination of the histidine with the central iron. The fit in Figure 2C gives the value (k_H) of 276 s^{-1} for the dimer and similar data for the monomer$_{S-H}$ yield k_H of 183.6 s^{-1}. These values are similar with those given in Table 2 and are comparable (within the same order of magnitude) with those previously reported [4,9,15]

In the monomer$_{S-S}$ we report differences in the observed rate constants between the slow phase of CO recombination following photolysis and CO combination seen by stopped-flow measurements. We explain this in terms of Scheme 1, in which there is a relaxed state, species iv, not populated in photolysis but the starting point for stopped-flow measurements. Combination with CO, measured by stopped-flow, to dimer$_{S-S}$ and monomer$_{S-H}$ is comparable to the observed rate constant of the slow phase of CO recombination monitored by flash photolysis (k_{slow}). This suggests that in these forms of the protein the transition to species iv from species iii effectively competes with the low value of k_{-H} and thus in static titrations and both types of kinetic experiments the hexacoordinate species with which we start observation is species iv.

The main conclusion that can be drawn from the values in Table 2 is that the histidine dissociation rate constant (k_{-H}) is approximately 1000 fold faster where the intramolecular disulfide bond is present compared with the monomer$_{S-H}$ or the dimer$_{S-S}$, between which there is no significant difference in k_{-H}. This is an important quantitative difference not previously reported, which affects the equilibrium constant (K_H) giving a value >2500 fold higher for the monomer$_{S-S}$ than the dimer$_{S-S}$ and monomer$_{S-H}$, compared to the previous reported difference of 13.3 fold [9]. In contrast the histidine association rate constants (k_H) are relatively insensitive to this protein structural element. Therefore, as previously discussed [7-9,14], the distal histidine dissociation rate is the controlling factor for exogenous ligand binding and this is regulated by the structural constraints imposed by the formation of the intramolecular disulfide bond. This coupling between the k_{-H} and the intramolecular disulfide bond is illustrated in Scheme 2. It may be noted that the dimer$_{S-S}$ is distinguished by two different factors, the considerably greater geminate recombination and the much lower overall K_D for CO as determined by static measurements (Figure 1). This lower K_D implies that species iv, the starting point for stopped-flow and static titration experiments, is relatively more stable in the dimer leading to a higher histidine affinity and thus lower CO affinity.

We have previously reported a similar situation where disulfide bonds regulate ligand binding in both the ferric and ferrous protein. The presence or absence of this disulfide bond in a cell would likely be associated with its overall redox state and this agrees with the postulated function as a signal protein in oxidative stress defense. Although we report the properties of the $dimer_{S\text{-}S}$ we consider it unlikely that this form of the protein is populated in the cell given the very low overall concentration of Cygb present (micromolar range) [9]. Instead we propose that it is the redox linked interconversion between $monomer_{S\text{-}S}$ and $monomer_{S\text{-}H}$ that endows the protein with this protective function.

Figure Legends

Figure 1. Titration of ferrous cytoglobin with CO

Dithionite-reduced $monomer_{S\text{-}S}$, $dimer_{S\text{-}S}$ and $monomer_{S\text{-}H}$ Cygb were titrated with CO (436 nm – 415 nm). The continuous line represents data points fitted to Equation 1.

Inset: Spectral changes on addition of saturating concentrations of CO to ferrous Cygb. Spectra shown are the dithionite-reduced $monomer_{S\text{-}S}$ (red) and the CO-$monomer_{S\text{-}S}$ (black). Spectra of the $dimer_{S\text{-}S}$ and $monomer_{S\text{-}H}$ were identical.

Figure 2. Time courses and difference spectra of the fast and slow phases of CO recombination to $monomer_{S\text{-}S}$ and $dimer_{S\text{-}S}$ following photolysis

(A&C) Normalized time courses monitored at 432 nm of the recombination of CO with $monomer_{S\text{-}S}$ (A) and $dimer_{S\text{-}S}$ (C) Cygb (5 µM) following flash photolysis at selected CO concentrations fitted to double exponentials

(B&D) The data points show the amplitude changes observed during the fast phase (blue triangle) and slow phase (red triangle) of recombination (32 µM CO) to $monomer_{S\text{-}S}$ (B) and $dimer_{S\text{-}S}$ (D) Cygb (5 µM) following flash photolysis monitored at selected wavelengths. The solid lines show the scaled static difference spectra between the ferrous-CO complex and hexacoordinated ferrous-Cygb (WT) as shown in green in panels B and D; the purple line in panel B shows the difference spectrum between the ferrous pentacoordinate Cygb species (H81Y) and the ferrous-CO complex (WT); the black line in panel D shows the difference spectrum of ferrous pentacoordinate (H81Y) Cygb and ferrous hexacoordinate Cygb (WT).

Figure 3. Kinetics of the recombination of CO to cytoglobin in the monomer$_{S\text{-}S}$, dimer$_{S\text{-}S}$ and monomer$_{S\text{-}H}$ forms following photolysis.

The time courses of CO recombination to cytoglobin were biphasic in all forms of the protein. The monomer$_{S\text{-}S}$ is represented with blue circles, dimer$_{S\text{-}S}$ in black triangles and monomer$_{S\text{-}H}$ in red diamonds. The observed rate constants of the fast phase are shown in (A) and were fitted linearly, the amplitude changes associated with this phase are shown in (B) and were fitted to standard hyperbola (Equation 2). The observed rates of the slow phase are shown in (C) and the associated amplitude changes of this phase are shown in (D). The monomer$_{S\text{-}S}$ is shown in blue, dimer$_{S\text{-}S}$ in black and monomer$_{S\text{-}H}$ in red.

Scheme 1. Mechanism of CO binding to ferrous cytoglobin

The kinetics of CO binding can be monitored by 2 different methods: CO recombination by flash photolysis (1) and CO combination to the bis-His complex by stopped-flow (iv). Upon laser illumination of the CO complex (i) the pentacoordinate form of the protein is generated (ii). There are two possible routes of CO recombination giving a biphasic time course. The second order process of CO recombination directly to the penta-coordinate haem (k_{CO}) represents the fast kinetics. The distal histidine can bind in a first order process (k_H) leading to a hexacoordinate form (iii). Subsequent binding of CO is then rate limited by the distal histidine dissociation rate (k_{-H}). We propose two forms of the hexacoordinate species of Cygb (iii and iv) where species iv is a relaxed form of species iii. In flash photolysis species iii is the dominant hexacoordinate form populated in the monomer$_{S\text{-}S}$. In the monomer$_{S\text{-}S}$ slower relaxation to species iv ($k_R < k_{-H}$) results in the hexacoordinate form that is the initial starting point for stopped-flow experiments accounting for the difference in CO combination kinetics monitored by stopped-flow or flash photolysis experiments. For the dimer$_{S\text{-}S}$ and monomer$_{S\text{-}H}$ species iii is a transiently populated species and both stopped-flow and flash photolysis start at species iv ($k_R > k_{-H}$).

Scheme 2. Illustration of the coupling between the disulfide bond and the distal histidine dissociation rate constant that links species ii and iii of Scheme 1

Adapted from Beckerson *et al.* 2015. The formation of a disulfide bond between C38 and C83 leads to a positional change in helices B and E altering the dissociation rate constant (k_{-H}) of the distal histidine (H81) from the iron in species iii. This change in k_{-H} (>1000 fold higher) leads to a more pentacoordinate-like protein resulting in faster rates of exogenous ligand binding. The association rate of the histidine is not greatly affected by the formation of this bond.

Cytoglobin conformer	Fast phase ($M^{-1}s^{-1}$) (k_{CO})	K (M) (CO concentration at Y = 0.5)	Slow phase ($M^{-1}s^{-1}$) (k_{slow})
$Monomer_{S-S}$	$7.14 \times 10^6 \pm 9.0 \times 10^4$	$7.30 \times 10^{-5} \pm 1.4 \times 10^{-5}$	$1.53 \times 10^6 \pm 2.0 \times 10^5$
$Dimer_{S-S}$	$2.49 \times 10^6 \pm 2.0 \times 10^3$	$9.37 \times 10^{-5} \pm 7.1 \times 10^{-5}$	$1.43 \times 10^3 \pm 3.0 \times 10^2$
$Monomer_{S-H}$	$2.53 \times 10^6 \pm 3.0 \times 10^5$	$1.34 \times 10^{-4} \pm 4.5 \times 10^{-5}$	$1.1 \times 10^3 \pm 3.0 \times 10^2$

Y = fraction of fast phase

K = phenomenological parameter denoting the [CO] at which half the total amplitude occurs in the fast phase

Table 1. Second order rate constants and K value of CO recombination of $monomer_{S-H}$, $dimer_{S-S}$ and $monomer_{S-H}$ cytoglobin following flash photolysis

Cytoglobin conformer	Histidine equilibrium constant (K_H)	Histidine on rate constant (k_H) (s^{-1})	Histidine off rate constant (k_{-H}) (s^{-1})
$Monomer_{S-S}$	$4.8 \pm 6.1 \times 10^{-1}$	$5.2 \times 10^2 \pm 1.0 \times 10^2$	$1.1 \times 10^2 \pm 2.6 \times 10^1$
$Dimer_{S-S}$	$1.8 \times 10^3 \pm 3.7 \times 10^2$	$2.3 \times 10^2 \pm 1.7 \times 10^2$	$1.3 \times 10^{-1} \pm 1.1 \times 10^{-1}$
$Monomer_{S-H}$	$2.0 \times 10^3 \pm 4.3 \times 10^2$	$3.3 \times 10^2 \pm 1.2 \times 10^2$	$1.7 \times 10^{-1} \pm 7.0 \times 10^{-2}$

K_H is the equilibrium constant calculated by k_H/k_{-H}.

Table 2. Values of the equilibrium kinetic parameters describing the model in Scheme 1

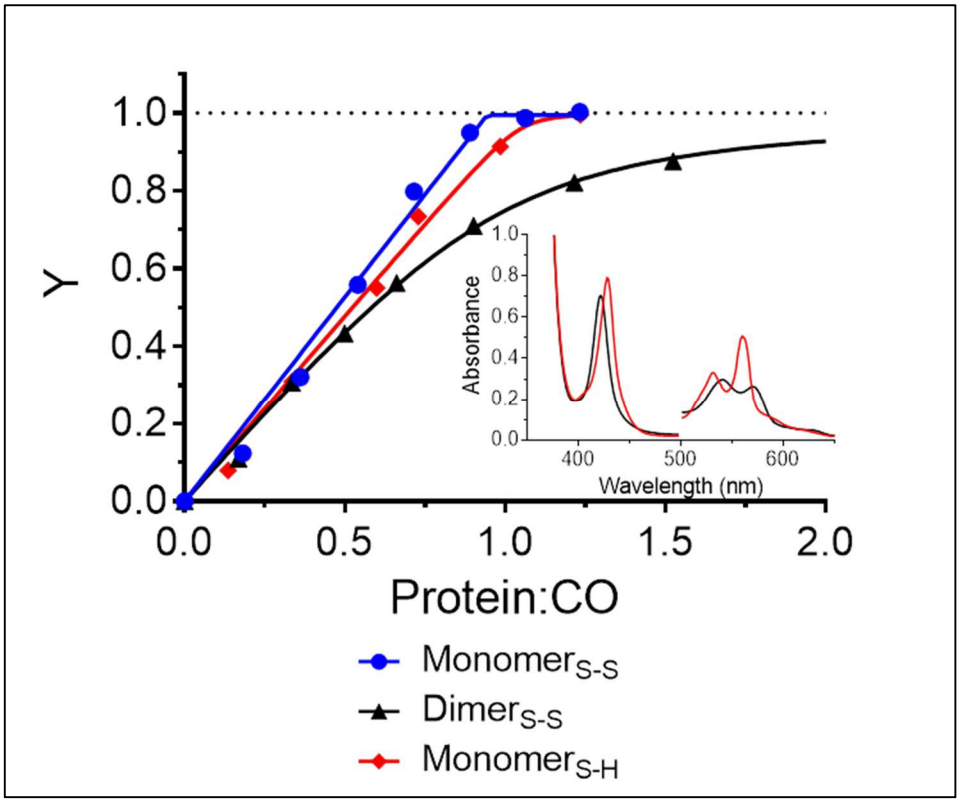
1.0
0.8
0.6
0.4
0.2
0.0
Y
0.0
0.5
1.0
1.5
2.0
Protein:CO
Absorbance
1.0
0.8
0.6
0.4
0.2
0.0
400
500
600
Wavelength (nm)
Monomer S-S
Dimer S-S
Monomer S-H

Figure 1.

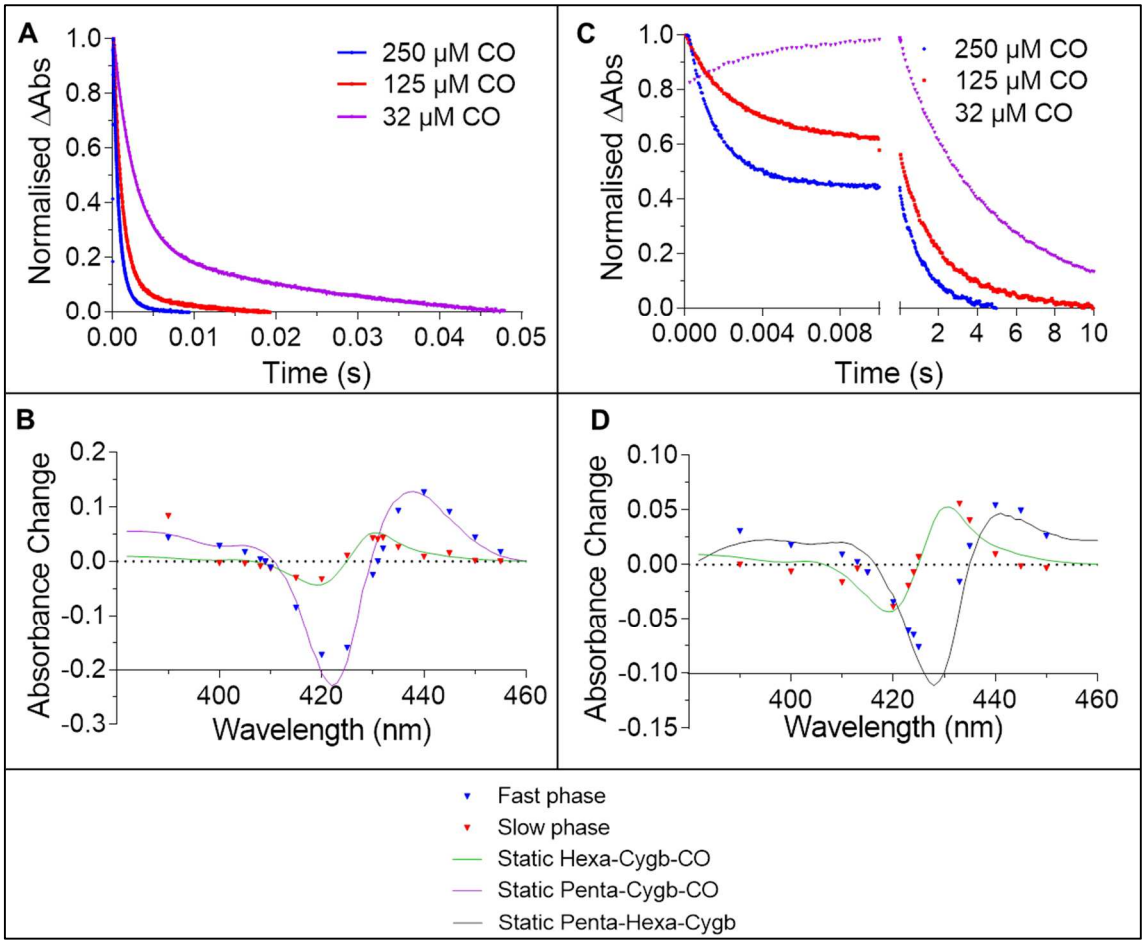
A
Normalised ΔAbs
1.0
0.8
0.6
0.4
0.2
0.0
0.00
0.01
0.02
0.03
0.04
0.05
Time (s)
250 μM CO
125 μM CO
32 μM CO
C
Normalised ΔAbs
1.0
0.8
0.6
0.4
0.2
0.0
0.000
0.004
0.008
2
4
6
8
10
Time (s)
250 μM CO
125 μM CO
32 μM CO
B
Absorbance Change
0.2
0.1
0.0
-0.1
-0.2
-0.3
400
420
440
460
Wavelength (nm)
D
Absorbance Change
0.10
0.05
0.00
-0.05
-0.10
-0.15
400
420
440
460
Wavelength (nm)
Fast phase
Slow phase
Static Hexa-Cygb-CO
Static Penta-Cygb-CO
Static Penta-Hexa-Cygb

Figure 2.

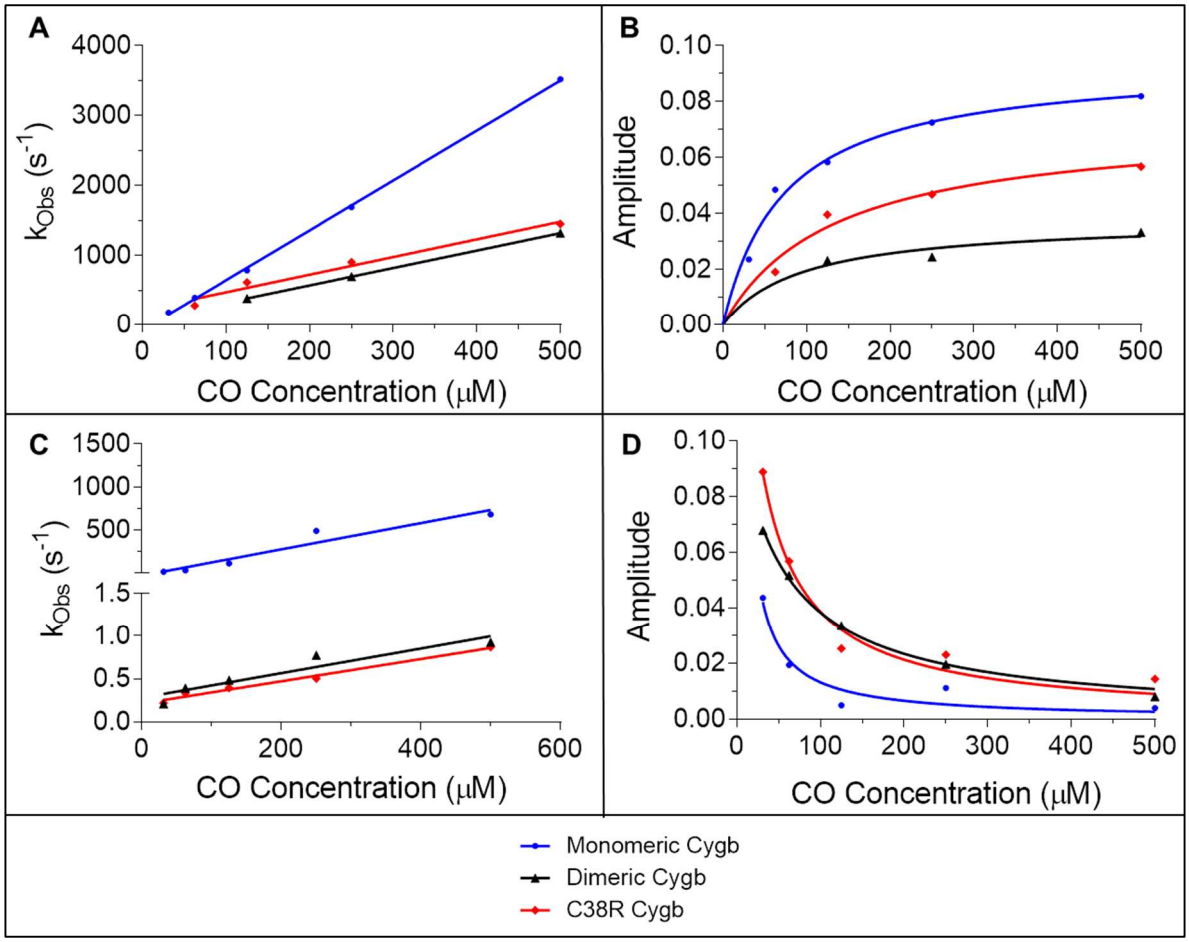
A
4000
3000
2000
1000
0
k_{Obs} (s^{-1})
0
100
200
300
400
500
CO Concentration (μM)
B
0.10
0.08
0.06
0.04
0.02
0.00
Amplitude
0
100
200
300
400
500
CO Concentration (μM)
C
1500
1000
500
1.5
1.0
0.5
0.0
k_{Obs} (s^{-1})
0
200
400
600
CO Concentration (μM)
D
0.10
0.08
0.06
0.04
0.02
0.00
Amplitude
0
100
200
300
400
500
CO Concentration (μM)
Monomeric Cygb
Dimeric Cygb
C38R Cygb

Figure 3.

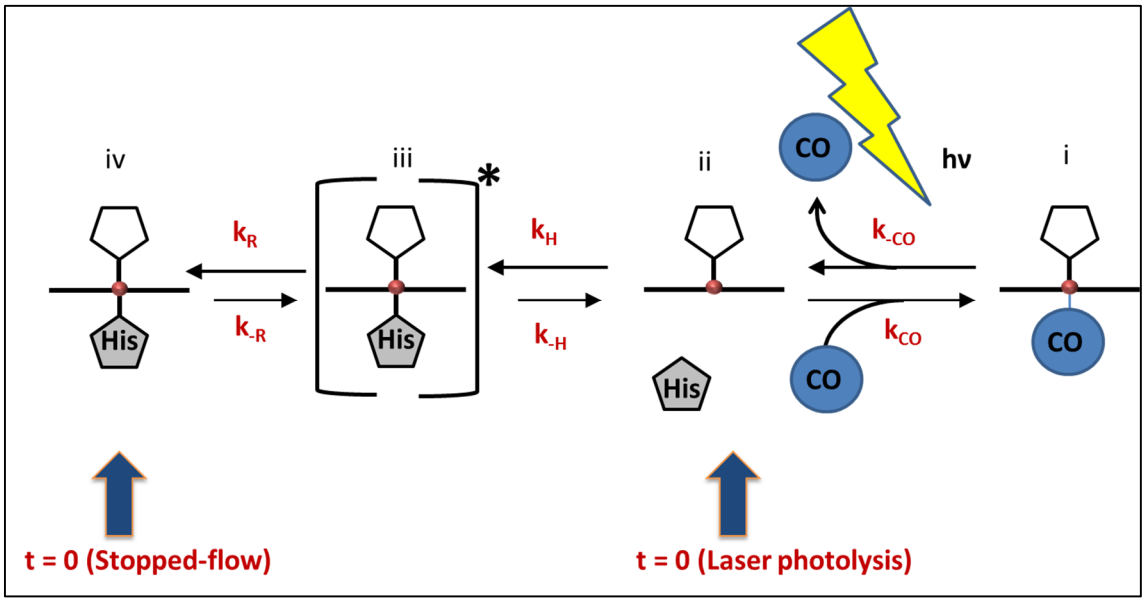

Scheme 1.

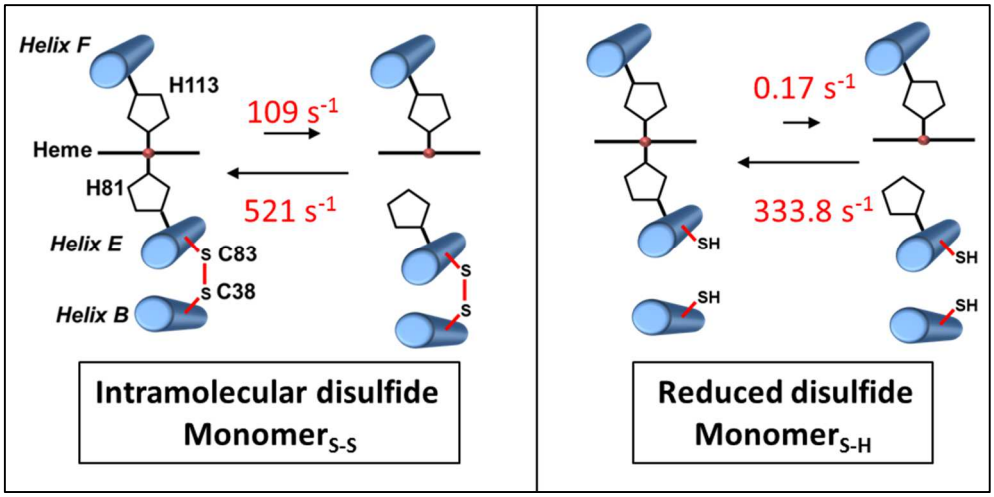

Scheme 2.

References

[1] Kawada, N., Kristensen, D.B., Asahina, K., Nakatani, K., Minamiyama, Y., Seki, S. and Yoshizato, K. (2001). Characterization of a Stellate Cell Activation-associated Protein (STAP) with Peroxidase Activity Found in Rat Hepatic Stellate Cells. Journal of Biological Chemistry 276, 25318-25323.

[2] Burmester, T., Ebner, B., Weich, B. and Hankeln, T. (2002). Cytoglobin: A Novel Globin Type Ubiquitously Expressed inVertebrate Tissues. Molecular Biology and Evolution 19, 416-421.

[3] Dewilde, S. et al. (2001). Biochemical Characterization and Ligand Binding Properties of Neuroglobin, a Novel Member of the Globin Family. Journal of Biological Chemistry 276, 38949-38955.

[4] Trent, J.T. and Hargrove, M.S. (2002). A Ubiquitously Expressed Human Hexacoordinate Hemoglobin. Journal of Biological Chemistry 277, 19538-19545.

[5] Sanctis, D.d., Dewilde, S., Pesce, A., Moens, L., Ascenzi, P., Hankeln, T., Burmester, T. and Bolognesi, M. (2004). Crystal Structure of Cytoglobin: The Fourth Globin Type Discovered in Man Displays Heme Hexa-coordination. Journal of Molecular Biology 336, 917-927.

[6] Sawai, H., Kawada, N., Yoshizato, K., Nakajima, H., Aono, S. and Shiro, Y. (2003). Characterization of the Heme Environmental Structure of Cytoglobin, a Fourth Globin in Humans. Biochemistry 42, 5133-5142.

[7] Trent, J.T., Hvitved, A.N. and Hargrove, M.S. (2001). A Model for Ligand Binding to Hexacoordinate Hemoglobins. Biochemistry 40, 6155-6163.

[8] Smagghe, B.J., Sarath, G., Ross, E., Hilbert, J.L. and Hargrove, M.S. (2006). Slow ligand binding kinetics dominate ferrous hexacoordinate hemoglobin reactivities and reveal differences between plants and other species. Biochemistry 45, 561-70.

[9] Lechauve, C., Chauvierre, C., Dewilde, S., Moens, L., Green, B.N., Marden, M.C., Célier, C. and Kiger, L. (2010). Cytoglobin conformations and disulfide bond formation. FEBS Journal 277, 2696-2704.

[10] Tsujino, H., Yamashita, T., Nose, A., Kukino, K., Sawai, H., Shiro, Y. and Uno, T. (2014). Disulfide bonds regulate binding of exogenous ligand to human cytoglobin. Journal of Inorganic Biochemistry 135, 20-27.

[11] Beckerson, P., Wilson, M.T., Svistunenko, D.A. and Reeder, B.J. (2015). Cytoglobin ligand binding regulated by changing haem-coordination in response to intramolecular disulfide bond formation and lipid interaction. Biochem J 465, 127-137.

[12] Hamdane, D. et al. (2003). The Redox State of the Cell Regulates the Ligand Binding Affinity of Human Neuroglobin and Cytoglobin. Journal of Biological Chemistry 278, 51713-51721.

[13] Reeder, B.J., Svistunenko, D.A. and Wilson, M.T. (2011). Lipid binding to cytoglobin leads to a change in haem co-ordination: a role for cytoglobin in lipid signalling of oxidative stress. Biochemical Journal 434, 482-492.

[14] Hargrove, M.S. (2000). A Flash Photolysis Method to Characterize Hexacoordinate Hemoglobin Kinetics. Biophysical Journal 79, 2733-2738.

[15] Gabba, M. et al. (2013). CO Rebinding Kinetics and Molecular Dynamics Simulations Highlight Dynamic Regulation of Internal Cavities in Human Cytoglobin. PLoS ONE 8, e49770.